Fabrication and Superconductivity of Ba$_{0.6}$K$_{0.4}$Fe$_2$As$_2$/Ag Wires and Tapes Using Mechanical Alloyed Precursor

X. Li, F. Wan, M.D. Sumption, E.W. Collings, C.S. Myers, and Z.X. Shi

Abstract—Conventional methods of Ba$_{0.6}$K$_{0.4}$Fe$_2$As$_2$ precursor preparation are complicated and expensive. In this paper, we describe the mechanical alloying of precursor by high-energy ball milling and its processing to wires and tapes. Our approach is to high-energy ball-mill a starting mixture of Ba and K pieces with Fe and As powders. The resultant powders are packed into an Ag sheath and reduced by groove rolling or flat rolling. Critical current density measurements were performed on un-sintered wire and tape, and compared to the results of measurements on wire and tape sintered at 750 °C for 12 h. We achieved 6.98×10^4 A/cm^2 at 4.2 K and self-field in the sintered tape. Our results indicate that the mechanical alloyed precursor and the resulting Ag-sheathed Ba$_{0.6}$K$_{0.4}$Fe$_2$As$_2$ wires and tapes are promising but require further development.

Index Terms—Critical current density, high-energy ball milling, iron-based superconductor, superconducting wire.

I. INTRODUCTION

IRON-BASED superconductors in wire and tape forms have their outstanding advantages, such as moderately high superconducting transition temperatures (T_c), high upper critical fields (H_{c2}), and, in some cases, the potential for strong vortex pinning [1]–[6]. Among the iron-based superconductor family, the 122-type compound is the most promising because of its high H_{c2}, and low anisotropy [1], [7]. Recently, the transport critical current density (J_c) of Sr-122 tape reached 0.1 MA/cm^2 at 10 T and 4.2 K [8]. It has been demonstrated that the micro-scale porosity observed in 122-type bulks causes a large reduction in the actual superconducting cross-sectional area producing a large decrease in the transport J_c [1], [7]. Thus, 122-type superconducting wires and tapes are usually fabricated by the *ex-situ* powder-in-tube (PIT) method in which pre-formed 122-type polycrystalline powder is used as precursor to avoid porosity arising from chemical reaction [1], [7].

The 122-type precursor is generally prepared by a one-step

X. Li and Z.X. Shi are with Department of Physics and Key Laboratory of MEMS of the Ministry of Education, Southeast University, Nanjing 211189, China (e-mail: lixionghm@hotmail.com).

X. Li, F. Wan, M.D. Sumption, E.W. Collings and C.S. Myers are with Center for Superconducting and Magnetic Materials, Department of Materials Science and Engineering, The Ohio State University, Columbus, OH 43210, USA.

PIT or two-step solid-state-reaction (SSR) method. For the one-step PIT method, a mixture of pure elements (Ba, K, Fe and As) is ball-milled by a planetary ball milling after which the as-milled powders are sealed in a Nb tube in preparation for sintering [1], [9]–[11]. Next, the sintered bulk is removed from the Nb tube and processed to wire/tape after ground by hand. In the case of the two-step SSR method, binary compounds such as B-As (B = Ba, Sr, K, Co, Fe or P) are first synthesized. Subsequently, these binary compounds are ground and mixed with the other pure elements according to the nominal composition and then sintered before being filled into a tube for wire drawing [5], [7]. Besides, to improve the homogeneity for the 122-type phase, the third step is usually taken. The sintered bulk is re-ground, re-mixed, and re-sintered. Obviously, such a complicated process and the high production cost of these methods are problems for large-scale industrial production. Hence, a scalable and low-cost method is particularly desirable.

Recently, a mechanical alloying method was developed to prepare the 122-type precursor [12]–[14]. A mixture of pure elements (A, K, Fe and As, A denotes alkali earth) is mechanical alloyed by high-energy ball milling. The high-energy ball milling initiates a self-sustaining reaction, resulting in the formation of the 122-type phase. Importantly, the mechanical alloyed precursor can be immediately used for wire fabrication. Therefore, in this paper, we report the fabrication and superconductivity of Ag-sheathed Ba$_{0.6}$K$_{0.4}$Fe$_2$As$_2$ wires and tapes using the mechanical alloyed precursor approach.

II. EXPERIMENTAL

Ba$_{0.6}$K$_{0.4}$Fe$_2$As$_2$/Ag wires with rectangular cross sections were fabricated by the *ex-situ* PIT method. Ba pieces (99.99%), K pieces (99.95%), Fe powder (99.99%) and As powder (99.99%) were used as the starting materials. Mixtures with a ratio of Ba:K:Fe:As = 0.6:0.4:2:2 were placed in an argon-filled stainless steel canister and then high-energy ball-milled (SPEX mill) for 4 h. The weight ratio of stainless steel balls to the mixture was about 10:1 [14]. Mechanical alloyed powder was loaded into a pure Ag tube of 4.6 mm OD and 2.7 mm ID. The composite was then cold worked into wires with various cross-sectional areas through groove rolling. The wires with cross-sectional areas of ~ 1.7 and 0.71 mm^2 will be referred as W$_1$ and W$_2$, respectively. To fabricate tapes, a multi-pass flat rolling process is employed. The as-fabricated wires and tapes were cut into short pieces. After that, some pieces were sealed

in evacuated quartz tubes, and sintered at 750 $^{\circ}$C for 12 h. Powder x-ray diffraction (XRD) pattern was measured using the $2\theta/\theta$ method with Cu Kα radiation. Magnetization measurements were performed using a Physical Property Measurement System (PPMS, Quantum Design). Microstructural and compositional investigations were performed by field emission scanning electron microscopy (SEM) equipped with energy dispersive x-ray spectroscopy (EDXS). Transport measurements of critical current (I_c) using a standard four probe method were carried out in transverse fields up to 10 T in pool-boiling liquid He at 4.2 K on samples 50 mm long with a gauge length of 5 mm. The transport J_c was calculated by dividing the I_c by the area of the core, and the electric field criterion for the transport measurements was 1 μV/cm.
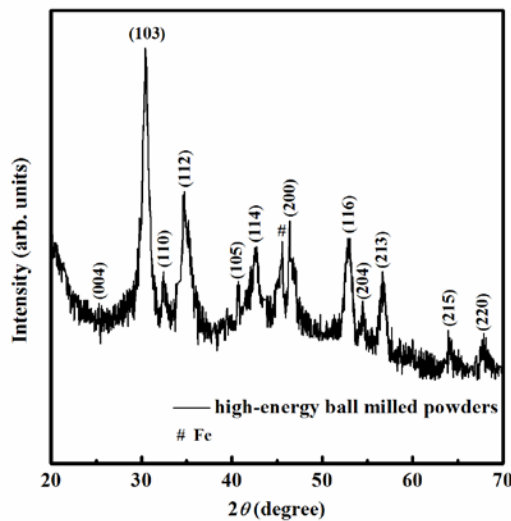

Fig. 1. XRD pattern of the high-energy ball-milled $Ba_{0.6}K_{0.4}Fe_2As_2$ powders. Numbers refer to the Miller index.

TABLE I
DETAILS OF SAMPLES

Samples	Cross-sectional areas of samples (mm^2)	Cross-sectional areas of superconducting cores (mm^2)
W_1 wire	1.7	0.336
W_2 wire	0.71	0.09
Un-sintered tape	0.842	0.24
Sintered tape	0.74	0.148

III.   RESULTS AND DISCUSSION

Fig. 1 shows the XRD pattern of the mechanical alloyed precursor powders. A crystalline $Ba_{0.6}K_{0.4}Fe_2As_2$ phase is formed, confirming that the high-energy ball milling not only mixes the powders but initiates a self-sustaining reaction [13], [14]. On the contrary, such a self-sustaining reaction does not take place during planetary ball milling, so long-time, high-temperature, sintering needs to be introduced [1], [15]. This sintering not only increases the production cost, but also restricts the use of some sheath materials, including Fe, Cu and brass, because these sheaths would react with the core during sintering [1], [14], [16]. Small amounts of Fe

impurities coming from the starting materials and/or ball milling media and canister may be present in the mechanical alloyed precursor; fortunately, Fe is one of the constituent
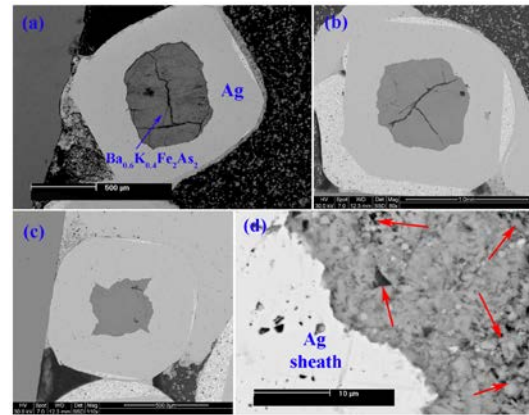

Fig. 2.   SEM images of the transverse cross sections of the (a) un-sintered W_1, (b) sintered W_1 and (c) sintered W_2. (d) Backscattered electron image of higher magnification of the sintered W_2.
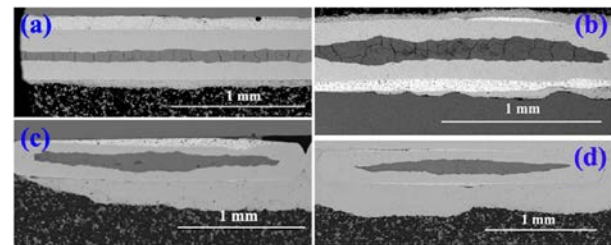

Fig. 3. SEM images of the (a) longitudinal and (b) transverse cross sections of the un-sintered tape, and (c) longitudinal and (d) transverse cross sections of the sintered tape.

elements of our final material. We can expect a better crystallization after the optimization of the high-energy ball milling process.

The SEM images presented in Fig. 2(a) – (c) show the transverse cross sections of un-sintered and sintered W_1, and sintered W_2, respectively. The core areas are ~ 0.336 mm^2 for W_1 and 0.09 mm^2 for W_2. As seen in Fig. 2(a), mechanical deformation during the groove rolling brings about obvious cracks in the un-sintered W_1. The comparison of Fig. 2(a) and (b) indicates that the cracks were reduced by sintering. The crack can be barely observed in the sintered W_2, which may due to its higher level of powder compaction. Fig. 2(d) shows a higher magnification backscattered electron image of the sintered W_2. It can be seen that the boundary between the Ag sheath and the $Ba_{0.6}K_{0.4}Fe_2As_2$ core is very clear, indicating no reaction between the Ag sheath and the core and confirming the chemical stability of Ag [1], [11]. However, for the Cu-sheathed $Ba_{0.6}K_{0.4}Fe_2As_2$ wires, obvious reaction layers with thicknesses of several μm were observed [14], [16]. Micro-scale porosity shown by red arrows in Fig. 2(d) is present in our sintered $Ba_{0.6}K_{0.4}Fe_2As_2$ wire. It is known that micro-scale porosity will contribute to weak link behavior at grain boundaries in the iron-based superconductors [1], [8], [14]. The effect of the micro-scale porosity on the transport J_c is discussed below. Fig. 3(a) – (d) shows the SEM images of the longitudinal and transverse cross sections of un-sintered and sintered tapes. The cracks were found in the un-sintered tapes

but healed for the sintered tape, as in the wires discussed above. The core areas of the un-sintered and sintered tapes from different passes of the flat rolling are about 0.24 and 0.148 mm^2. Details of samples are listed in Table I.

As shown in Fig. 4(a) – (f), the good homogeneity of the sintered W_2 is confirmed by EDXS mapping based on SEM, which demonstrates that the element distribution of
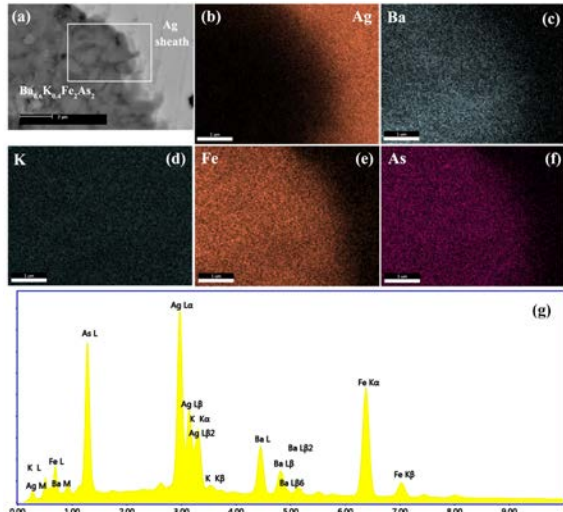

Fig. 4. (a) SEM image of an enlarged region for the sintered W_2. SEM - EDXS mapping images of (b) Ag, (c) Ba, (d) K, (e) Fe and (f) As for the sintered W_2. (g) EDXS analysis for the cross section of the sintered W_2.

$Ba_{0.6}K_{0.4}Fe_2As_2$ phase is homogeneously dispersed in the core. In addition, Ba, Fe and As elements, detected locally in the core area, almost completely disappear at the border of the Ag sheath. The slight diffusion of K into the Ag sheath noted in K mapping was also seen in some reported results [16], [17]. Since the area for the EDXS mapping is small (e.g. 5.14 × 3.9 μm^2), the slight diffusion of K can be resolved. The composition of the sintered W_2 by EDXS analysis in Fig. 4(g) is $Ba_{0.52}K_{0.48}Fe_2As_{2.07}$.

Because of the obvious cracks in the un-sintered and sintered W_1, and the un-sintered tape, magnetization measurements were only performed on the sintered W_2 and tape. The temperature dependences of zero-field-cooled (ZFC) and field-cooled (FC) magnetization for the sintered W_2 and tape are plotted in Fig. 5. The sintered W_2 and tape are superconductive as indicated by the onset of diamagnetism with decreasing temperature. Secondly, the T_c of ~ 31 K determined by the onset of the diamagnetic signal is nearly the same as that of the sintered W_2 and tape. This value of T_c of ~ 31 K is close to the reported results and in accordance with the actual composition by EDXS [1], [14]. Moreover, the susceptibility values above T_c for the sintered W_2 and tape are small, indicating a very low concentration of magnetic impurities such as FeAs and Fe in both samples. On the other hand, the sintered tape shows a sharper superconducting transition than the sintered W_2, which indicates a better homogeneity. In addition, compared to the sintered W_2, the susceptibility value at 5 K for the sintered tape is smaller, so the superconducting volume fraction of the sintered tape is

larger. Moreover, as shown in the FC branches, the sintered tape has a higher Meissner fraction than the sintered W_2, suggesting improved connectivity [14].
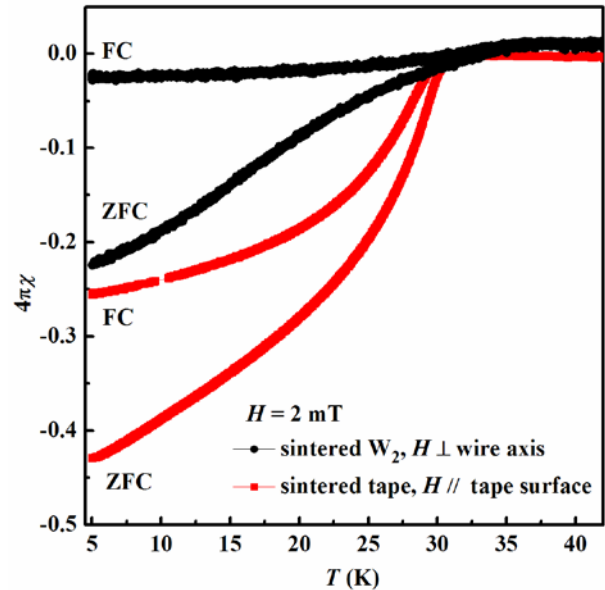

Fig. 5. Temperature dependence of the magnetic susceptibility of the sintered W_2 and tape.
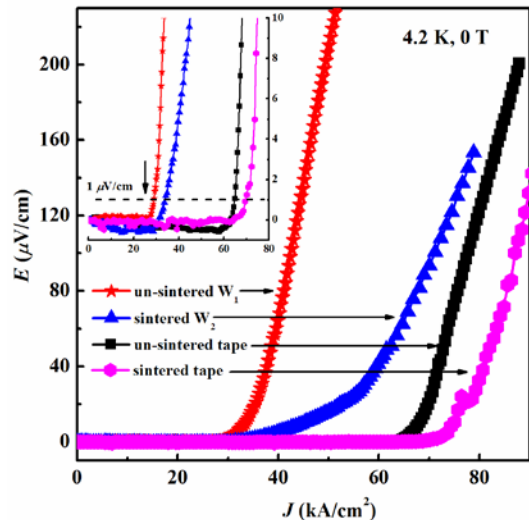

Fig. 6. The self-field $E–J$ curves of the un-sintered W_1 and tape, and the sintered W_2 and tape. The inset presents the details of the transition.

Transport measurements of I_c at 4.2 K were performed up to 10 T on the sintered W_2 and tape. The un-sintered W_1 and tape were measured for comparison. The self-field current–voltage ($E–J$) curves of all samples are plotted in Fig. 6. All self-field $E–J$ curves show clear transitions from a zero resistance state to a resistive state. It is interesting that the un-sintered W_1 and tape also exhibit transport J_cs, to the best of our knowledge this is the first report of a transport J_c in un-sintered samples. The transport J_c of un-sintered samples further confirms the formation and crystallization of $Ba_{0.6}K_{0.4}Fe_2As_2$ during high-energy ball milling. For the un-sintered W_1 and tape, and the sintered W_2 and tape, transport J_cs (at 4.2 K and self-field) are $2.9×10^4$, $6.5×10^4$, $3.39×10^4$ and $6.98×10^4$ A/cm^2 (I_c is 97.3,

155.3, 30.52 and 103.28 A), respectively. These values of the self-field transport J_cs of our samples are close to the literature [1], [14]. Compared to the sintered W_2, the higher self-field transport J_c of the sintered tape is in accordance with their
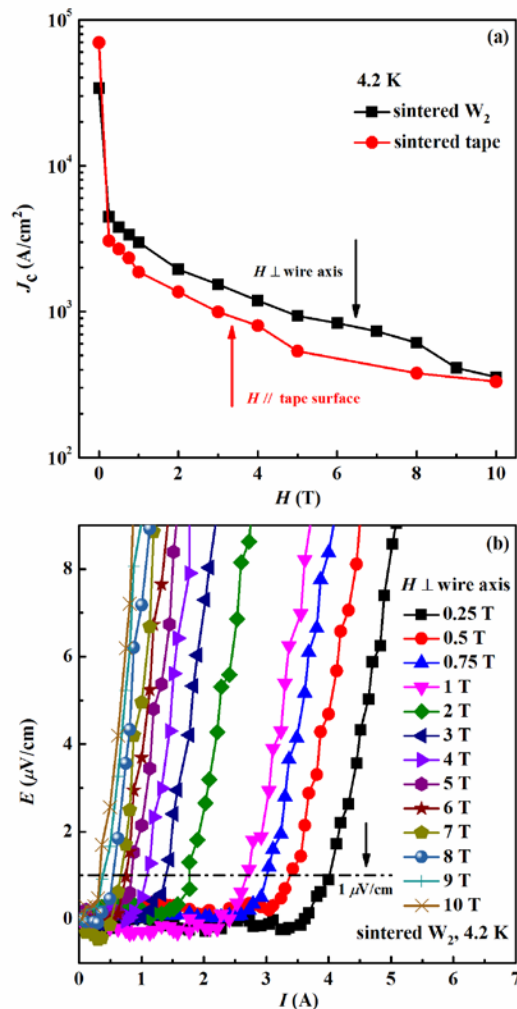

Fig. 7. (a) Magnetic field dependence of transport J_c at 4.2 K for the sintered W_2 and tape. (b) The $I–V$ characteristics of the sintered W_2 at 4.2 K up to 10 T.

magnetization measurements results discussed above. Moreover, the self-field transport J_cs of the sintered W_2 and tape are respectively similar to those of the un-sintered ones, indicating that sintering has little effect on intra-grain superconductivity. Besides, the transport J_c (4.2 K and self-field) of ~ 3.39×10^4 A/cm^2 of our sintered W_2 is higher than that of the reported Cu-sheathed $Ba_{0.6}K_{04}Fe_2As_2$ wire ~ 1.5 $\times 10^4$ A/cm^2 because of the greater chemical stability of Ag than Cu [14].

Transport J_c vs B for the sintered W_2 and tape is shown in Fig. 7(a). Fig. 7(b) presents the $I–V$ characteristics of the sintered W_2 at 4.2 K from 0.25 to 10 T. Both the un-sintered W_1 and tape showed resistive behavior at the minimum field of our transport J_c measuring system of 0.25 T (not shown) due to the cracks. Sintering of both the sintered W_2 and tape enabled the transport supercurrent in field of up to 10 T, suggesting the improvement of inter-grain supercurrent. Besides, for the reported Cu-sheathed $Ba_{0.6}K_{0.4}Fe_2As_2$ wires,

intergranular coupling deteriorated as a result of Cu doping, so no transport J_c was observed even at 0.25 T [14]. Therefore, the significant enhancement of the transport J_c under magnetic field in our Ag-sheath samples further confirms that the Ag sheath is appropriate for the fabrication of $Ba_{0.6}K_{0.4}Fe_2As_2$ wire/tape. However, the transport J_c of the sintered W_2 and tape sharply drops after a magnetic field of 0.25 T is applied, indicating serious weak-link behavior. Various factors contribute to the weak-link behavior: grain boundary misorientation, micro-scale porosity, and impurities [1], [8], [14]. Although the present samples have weak-link problems, we have been the first to demonstrate the fabrication of $Ba_{0.6}K_{0.4}Fe_2As_2$/Ag wires and tapes using the mechanical alloyed precursor, that are able to carry transport supercurrents in field of up to 10 T. Furthermore, we can expect a further enhancement of the transport J_c in our $Ba_{0.6}K_{04}Fe_2As_2$/Ag wires/tapes after improving inter-grain connectivity [1], [8], [14].

IV. CONCLUSION

We report the preparation of the mechanical alloyed $Ba_{0.6}K_{0.4}Fe_2As_2$ precursor by high-energy ball milling. The mechanical alloyed precursor was successfully processed to Ag-sheathed wires and tapes by the *ex-situ* PIT method for the first time. The T_c based on magnetization measurements for the sintered wire (1.7 mm^2) and tape was about 31 K. The largest transport J_c observed on the sintered tape was about 6.98×10^4 A/cm^2 at 4.2 K and self-field. Both the sintered wire and tape still carried supercurrent in field of up to 10 T. The mechanical alloyed precursor is promising for 122-type wire/tape development.

REFERENCES

[1]   Y. Ma, "Progress in wire fabrication of iron-based superconductors," *Supercond. Sci. Technol.*, vol. 25, no. 11, Nov. 2012, Art. no. 113001.
[2]   X. Li, J. X. Liu, S. N. Zhang, L. J. Cui, and Z. X. Shi, "Fabrication of FeSe0.5Te0.5 superconducting wires by an ex situ powder-in-tube method," *J. Supercond. Nov. Magn.*, vol. 29, no. 7, pp. 1755-1759, Jul. 2016.
[3]   S. Pyon, Y. Yamasaki, H. Kajitani, N. Koizumi, Y. Tsuchiya, S. Awaji, K. Watanabe, and T. Tamegai, "Effects of drawing and high-pressure sintering on the superconducting properties of (Ba,K)Fe2As2 powder-in-tube wires," *Supercond. Sci. Technol.*, vol. 28, no. 12, Dec. 2015, Art. no. 125014.
[4]   X. Li, Y. Zhang, F. Yuan, J. Zhuang, Z. Cao, X. Xing, W. Zhou, and Z. Shi, "Fabrication of Nb-sheathed FeSe0.5Te0.5 tape by an ex-situ powder-in-tube method," *J. Alloys Compd.*, vol. 664, pp. 218-222, Apr. 2016.
[5]   T. Tamegai, S. Pyon, Y. Tsuchiya, H. Inoue, N. Koizumi, and H. Kajitani, "Effects of high-pressure sintering on critical current density in (Ba,K)Fe2As2 PIT wires," *IEEE Trans. Appl. Supercond.*, vol. 25, no. 3, Jun. 2015, Art. no. 7300504.
[6]   A. Malagoli, E. Wiesenmayer, S. Marchner, D. Johrendt, A. Genovese, and M. Putti, "Role of heat and mechanical treatments in the fabrication of superconducting Ba0.6K0.4Fe2As2 ex situ powder-in-tube tapes," *Supercond. Sci. Technol.*, vol. 28, no. 9, Sep. 2015, Art. no. 095015.
[7]   C. Dong, C. Yao, H. Lin, X. Zhang, Q. Zhang, D. Wang, Y. Ma, H. Oguro, S. Awaji, and K. Watanabe, "High critical current density in textured Ba-122/Ag tapes fabricated by a scalable rolling process," *Scripta Mater.*, vol. 99, pp. 33-36, Apr. 2015.
[8]   X. Zhang, C. Yao, H. Lin, Y. Cai, Z. Chen, J. Li, C. Dong, Q. Zhang, D. Wang, Y. Ma, H. Oguro, S. Awaji, and K. Watanabe, "Realization of practical level current densities in Sr0.6K0.4Fe2As2 tape conductors for

high-field applications," *Appl. Phys. Lett.*, vol. 104, no. 20, May. 2014, Art. no. 202601.

[9]   Z. Gao, L. Wang, C. Yao, Y. Qi, C. Wang, X. Zhang, D. Wang, C. Wang, and Y. Ma, "High transport critical current densities in textured Fe-sheathed Sr1-xKxFe2As2+Sn superconducting tapes," *Appl. Phys. Lett.*, vol. 99, no. 24, Dec. 2011, Art. no. 242506.

[10] Z. Gao, K. Togano, A. Matsumoto, and H. Kumakura, "Achievement of practical level critical current densities in Ba1-xKxFe2As2/Ag tapes by conventional cold mechanical deformation," *Sci. Rep.*, vol. 4, Feb. 2014, Art. no. 4065.

[11] C. Yao, H. Lin, Q. Zhang, X. Zhang, D. Wang, C. Dong, Y. Ma, S. Awaji, and K. Watanabe, "Critical current density and microstructure of iron sheathed multifilamentary Sr1-xKxFe2As2/Ag composite conductors," *J. Appl. Phys.*, vol. 118, no. 20, Nov. 2015, Art. no. 203909.

[12] J. D. Weiss, C. Tarantini, J. Jiang, F. Kametani, A. A. Polyanskii, D. C. Larbalestier, and E. E. Hellstrom, "High intergrain critical current density in fine-grain (Ba0.6K0.4)Fe2As2 wires and bulks," *Nat. Mater.*, vol. 11, no. 8, pp. 682-685, Aug. 2012.

[13] J. D. Weiss, J. Jiang, A. A. Polyanskii, and E. E. Hellstrom, "Mechanochemical synthesis of pnictide compounds and superconducting Ba0.6K0.4Fe2As2 bulks with high critical current density," *Supercond. Sci. Technol.*, vol. 26, no. 7, Jul. 2013, Art. no. 074003.

[14] Y. Ding, G. Z. Li, Y. Yang, C. J. Kovacs, M. A. Susner, M. D. Sumption, Y. Sun, J. C. Zhuang, Z. X. Shi, M. Majoros, and E. W. Collings, "Effects of cold high pressure densification on Cu sheathed Ba0.6K0.4Fe2As2 superconducting wire," *Physica C*, vol. 483, pp. 13-16, Dec. 2012.

[15] H. Lin, C. Yao, X. P. Zhang, H. T. Zhang, D. L. Wang, Q. J. Zhang, Y. W. Ma, S. Awaji, and K. Watanabe, "Strongly enhanced current densities in Sr0.6K0.4Fe2As2 + Sn superconducting tapes," *Sci. Rep.*, vol. 4, Mar. 2014, Art. no. 4465.

[16] H. Lin, C. Yao, H. Zhang, X. Zhang, Q. Zhang, C. Dong, D. Wang, and Y. Ma, "Large transport J(c) in Cu-sheathed Sr0.6K0.4Fe2As2 superconducting tape conductors," *Sci. Rep.*, vol. 5, Jun. 2015, Art. no. 11506.

[17] H. Lin, C. Yao, X. P. Zhang, H. T. Zhang, Q. J. Zhang, D. L. Wang, and Y. W. Ma, "Enhanced transport critical current density in textured Sr0.6K0.4Fe2As2 + Ag tapes by an intermediate sintering process of precursors," *Physica C*, vol. 490, pp. 37-42, Jul. 2013.